



Autobrecciation and fusing of mafic magma preceding explosive eruptions

Aaron A. Marshall¹, Michael Manga², Brittany D. Brand¹ and Benjamin J. Andrews³

¹Department of Geosciences, Boise State University, 1910 University Drive, Boise, Idaho 83725, USA

²Department of Earth and Planetary Science, University of California–Berkeley, McCone Hall, Berkeley, California 94720, USA

³Global Volcanism Program, National Museum of Natural History, Smithsonian Institution, 10th Street and Constitution Avenue NW, Washington, D.C. 20560, USA

ABSTRACT

Bubble and crystal textures evolve during magma ascent, altering properties that control ascent such as permeability and viscosity. Eruption style results from feedbacks between ascent, bubble nucleation and growth, microlite crystallization, and gas loss, all processes recorded in pyroclasts. We show that pyroclasts of the mafic Curacautín ignimbrite of Llaima volcano, Chile, record a history of repeated autobrecciation, fusing, and crystallization. We identified pyroclasts with domains of heterogeneous vesicle textures in sharp contact with one another that are overprinted by extensive microlite crystallization. Broken crystals with long axes (l) >10 μm record fragmentation events during the eruption. A second population of unbroken microlites with $l \leq 10$ μm overprint sutures between fused domains, suggesting the highly crystalline groundmass formed at shallow depths after autobrecciation and fusing. Nearly all pyroclasts contain plutonic and ancestral Llaima lithics as inclusions, implying that fusing occurs from a few kilometers depth to as shallow as the surface. We propose that Curacautín ignimbrite magma autobrecciated during ascent and proto-pyroclasts remained melt rich enough to fuse together. Lithics from the conduit margins were entrained into the proto-pyroclasts before fusing. Autobrecciation broke existing phenocrysts and microlites; rapid post-fusing crystallization then generated the highly crystalline groundmass. This proposed conduit process has implications for interpreting the products of mafic explosive eruptions.

INTRODUCTION

The textural properties of erupted magmas and their associated deposits record conduit ascent dynamics and eruption mechanics, in particular the processes that lead to crystallization, gas loss, and fragmentation. For example, bubble textures in mafic magmas inform on the state of magmatic volatiles at the time of eruption (Valdivia et al., 2022), microlites are used to investigate magma ascent rates and rheological evolution (Vona et al., 2011; Arzilli et al., 2019), broken crystals record fragmentation and healing of melt (Cordonnier et al., 2012; Taddeucci et al., 2021), and deposit granulometry records fragmentation style and efficiency (White and Valentine, 2016). The interplay of bubble and crystalli-

zation dynamics, magma ascent, and gas loss gives rise to the diversity of eruption styles (Cassidy et al., 2018).

We examined pyroclast (clast) textures from the mafic Curacautín ignimbrite of Llaima volcano, Chile. We argue that domains of heterogeneous textures and entrained lithic fragments within clasts reflect episodes of autobrecciation and fusing of magma during ascent. In addition, size-restricted fractured plagioclase microlites suggest distinct episodes of crystallization, which has implications for using crystal size distributions to constrain decompression rates. These textures challenge our understanding of mafic explosive volcanism and impart a need for scrutinizing potentially overlooked pyroclast textures.

The Curacautín Eruption

The Curacautín ignimbrite is a 4.0–4.5 km^3 (dense-rock equivalent) unwelded basaltic andesite ignimbrite that erupted at ca. 12.6 ka from Llaima volcano, Chile (Marshall et al., 2022). Curacautín ignimbrite clasts exhibit two vesicle populations: a polylobate, tortuous vesicle network of 99% pore connectivity; and a second population of smaller, micrometer-scale, isolated vesicles (Fig. 1; Valdivia et al., 2022). The groundmass contains high microlite number densities and little glass. Recent studies suggest the eruption was the result of brittle fragmentation of a rapidly ascending, largely non-degassed magma (Marshall et al., 2022; Valdivia et al., 2022).

METHODS

We collected bulk Curacautín ignimbrite deposits and hand samples in the field and selected sieved clasts for further investigation. We used clast textures to constrain conduit processes during the eruption. High-magnification images were acquired using a tabletop scanner, scanning electron microscopy, and X-ray computed microtomography (μCT). Marshall et al. (2022) measured plagioclase microlite number densities, and Valdivia et al. (2022) computed crystal size distributions. We fit regressions to plagioclase crystal size distributions for size populations with long axes (l) ≤ 10 μm and >10 μm (see extended methods in the Supplemental Material¹).

RESULTS

Domains of heterogeneous vesicle textures exist in all hand samples, 86% of thin sections

¹Supplemental Material. Detailed sampling methods and locations, stratigraphic descriptions for samples analyzed in this study, operating conditions for sample imaging, crystal size distribution analyses of Valdivia et al. (2022), and Pearson coefficients for regressions in Figure 3. Please visit <https://doi.org/10.1130/GEOLOGYS.20164283> to access the supplemental material, and contact editing@geosociety.org with any questions.

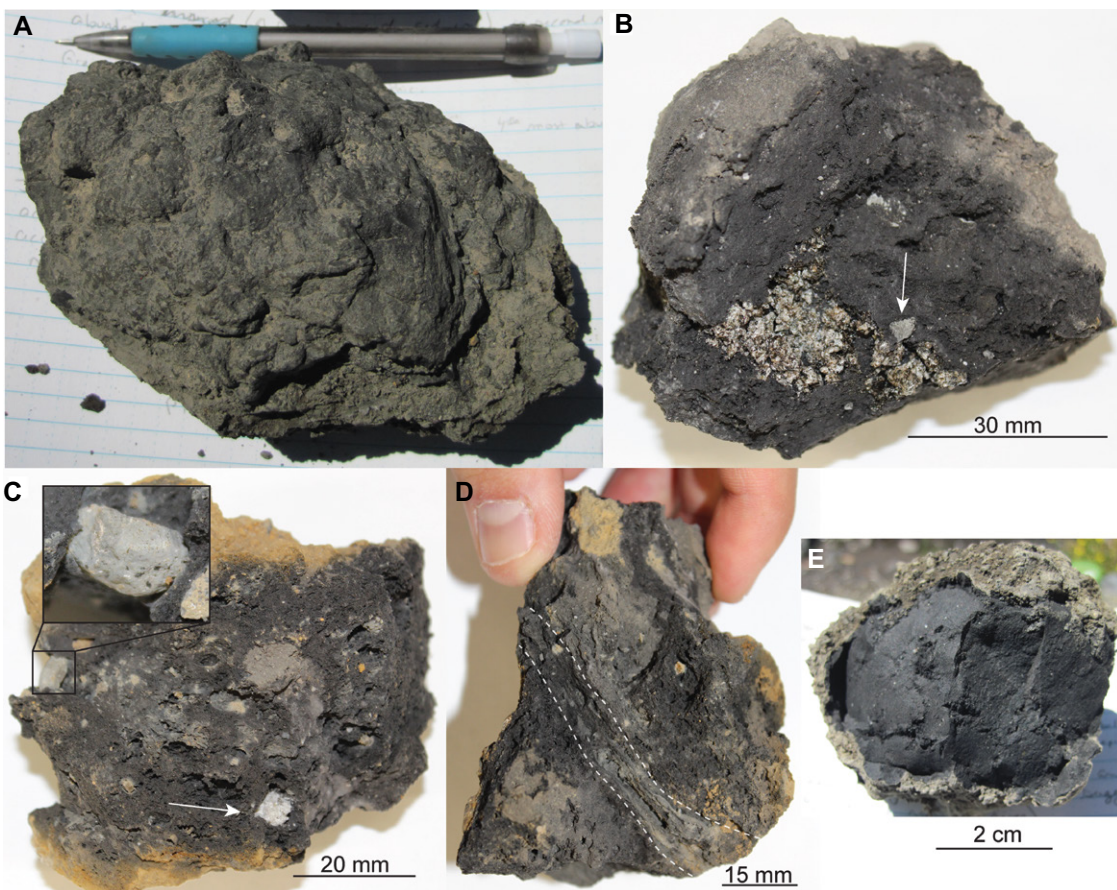


Figure 1. Microscale Curacautín (Chile) ignimbrite clast textures in thin section captured in plain polarized light. (A) Block consisting of agglomerated pyroclasts (Marshall et al., 2022). (B) Small block that contains crystal mush and intermediate lavas (white arrow). (C) Block with dioritic and intermediate lava lithics. (D) Flow banding between two domains of non-sheared magma (dotted white lines). (E) Dense, jointed clast or cored bomb (Sottili et al., 2010).

(54 of 63), and 53% of μ CT data sets (25 of 47) (Figs. 2A–2F). Some domains are separated by void space but most commonly are in sharp contact with one another. When these domains are in sharp contact, the groundmass across both domains is characterized by high micro-lite crystallinities of plagioclase, pyroxene, olivine, and Fe-Ti oxides and 29%–54% glass (Figs. 2D–2F). We were unable to collect glass compositions across fused domains because the groundmass of all clasts is too microlite rich. We identified entrained lithics of plutonic rocks and mafic to intermediate lavas in all hand samples and 92% of our thin sections and μ CT data sets (101 of 110). Lithics are mostly medium ash to fine lapilli in size (Figs. 1B, 1C, 2B, and 2C). We observe broken phenocrysts and microlites at high magnifications (Figs. 2G–2I).

DISCUSSION

Crystallization times (τ) inferred from crystal size distributions (Fig. 3) suggest disequilibrium crystallization of microlites and, thus, rapid ascent (Valdivia et al., 2022). Increased magma bulk viscosity and the abundant microlites confined bubbles during expansion, leading to the convoluted, but mostly connected, vesicle network. Bubble number densities of $1.1\text{--}2.3 \times 10^3 \text{ mm}^{-3}$ and permeabilities of $0.3\text{--}6 \times 10^{-12} \text{ m}^2$ (Valdivia et al., 2022) are similar to those of other volatile-driven mafic explosive eruptions,

such as the 60 ka Fontana Lapilli basalt and Masaya Triple Layer eruptions (Nicaragua; Constantini et al., 2009; Bamber et al. 2020), the 122 BCE Etna eruption (Italy; Coltellini et al., 1998; Houghton et al., 2004; Sable et al., 2006; Moitra et al., 2013), the 1886 CE Tarawera eruption (New Zealand; Carey et al., 2007; Sable et al., 2009; Schauroth et al., 2016), and mafic ignimbrites of the Roman magmatic province (Giordano et al., 2010; Vinkler et al., 2012). Valdivia et al. (2022) estimated a minimum average decompression rate for the Curacautín ignimbrite eruption of 1.4 MPa s^{-1} in the upper conduit. These results further highlight the role of rapid ascent for driving explosive mafic volcanism (Szramek et al., 2006; Moitra et al., 2018; Arzilli et al., 2019).

Curacautín ignimbrite clast textures record repeated episodes of autobrecciation and/or fragmentation, particle recapture and fusing, and further fragmentation within the conduit and during the eruption. The strongest evidence for autobrecciation and recapture are the heterogeneous vesicle domains within clasts (Fig. 2). Here, autobrecciation represents the shear-induced tearing of magma as it ascends, analogous to the processes in a'a flows (Fig. 4). Fragmentation, the breakup of magma into discrete pieces, may occur simultaneously due to gas overpressure and/or localized phreatomagmatic activity (Gonnermann, 2015). Like ash

sintering during rhyolitic eruptions (Gardner et al., 2017; Wadsworth et al., 2020), fusing is the welding together of melt-rich particles above the glass transition temperature within the conduit prior to eruption. Unlike sintering, however, fused clasts retain their original porosity. Fused domains exist throughout clasts, suggesting this process occurred when proto-clasts were still melt rich and hot enough to fully fuse prior to climactic fragmentation. The lack of deformation within fused clasts suggests autobrecciation likely occurred prior to final fragmentation into a turbulent gas-pyroclast mixture; however, we recognize that fusing may have occurred in this phase as well. We identified fused clasts from the micrometer scale to as large as fine block in size, the latter being the upper limit of sizes preserved in accessible Curacautín ignimbrite deposits, implying this process occurred over a range of spatial scales (Figs. 1 and 2). The ubiquity of fusing suggests that autobrecciation may have extended across the entire conduit (Fig. 4).

The contacts between fused domains are overprinted with extensive microlite crystallization (Figs. 2 and 4), indicating that the finest microlite population (long axis $l < 10 \mu\text{m}$) formed post-fusing and therefore post-initial fragmentation (Fig. 3). Additionally, while larger plagioclase microlites are commonly broken, microlites with $l < 10 \mu\text{m}$ are largely intact, further indicating crystallization post-fusing.

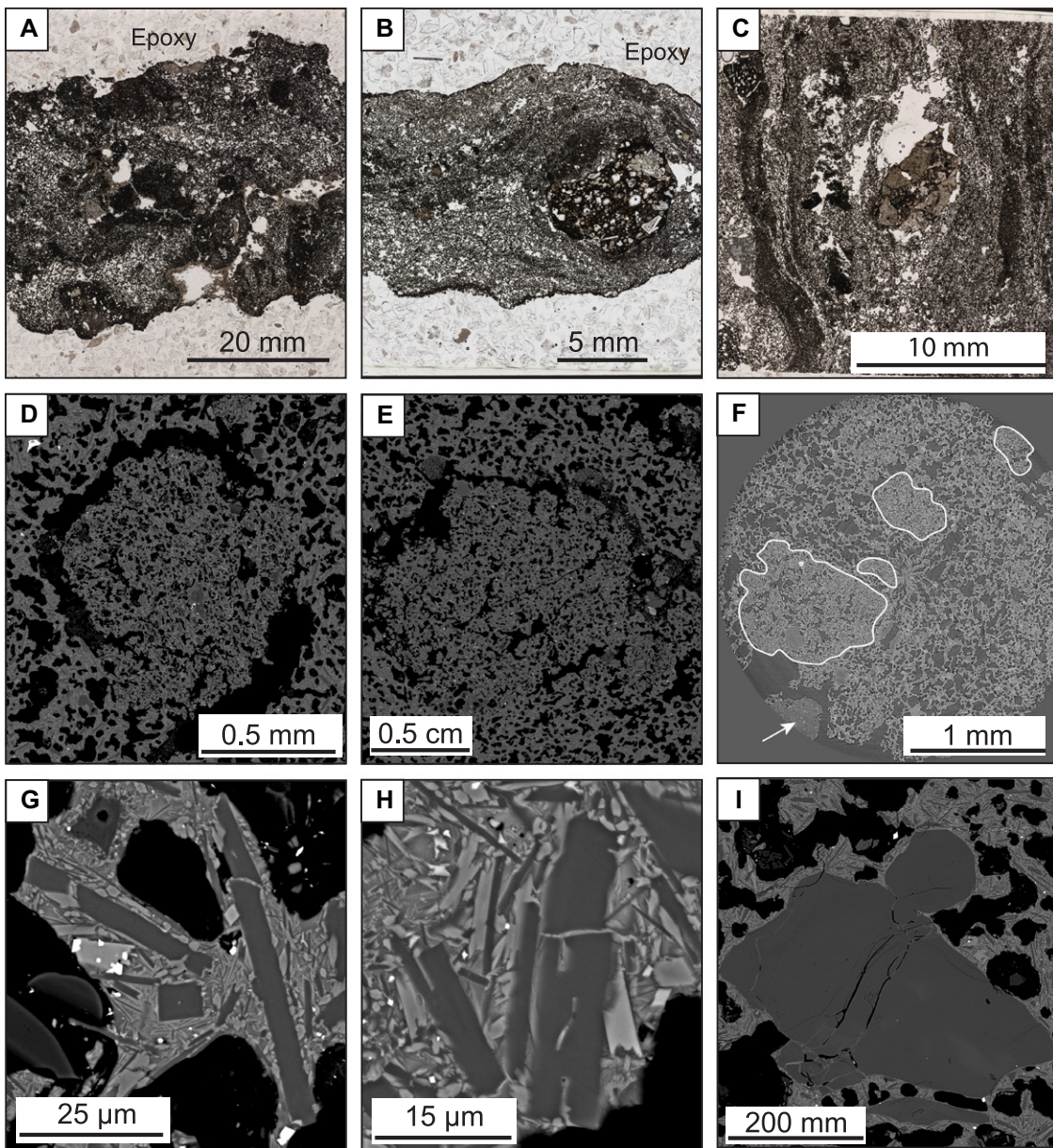


Figure 2. Microscale Curacautín (Chile) ignimbrite clast textures. (A) Multiple contrasting vesicle texture domains. (B) Flow banding around a lithic inclusion. (C) Layering of contrasting domains and lithic inclusion. (D,E) Scanning electron microscopy (SEM) images of fused clasts. (F) Tomography scan of a clast with multiple fused domains (white polygons) and lithic inclusions (arrow). Fused domains are pervasive in Curacautín ignimbrite clasts and commonly trapped in the clast interior. (G–I) SEM images of fractured plagioclase microlites surrounded by smaller, unbroken microlites.

Subtracting the $l < 10 \mu\text{m}$ plagioclase population reduces the plagioclase fraction from 29%–44% to 17%–29% and increases the glass content from 25%–54% to 40%–66% (Table S1 in the Supplemental Material), which may have enabled fusing. This interpretation is further supported by two separate regressions in plagioclase crystal size distributions (Fig. 3). The smallest size population likely formed after the cycles of autobrecciation and fusing, perhaps even syneruptively. Rapid microlite crystallization is expected in the shallow conduit where undercooling is highest and would be further enhanced by the increased rate of gas loss following fragmentation (Hammer, 2004, 2008).

The pervasive inclusion of lithics within Curacautín ignimbrite clasts allows us to constrain the depth of autobrecciation (Fig. 4). We suggest that lithics were entrained via a combination of shear-induced erosion, phreatic, and/or

phreatomagmatic processes along conduit walls. While phreatic or phreatomagmatic activity may have played a role in fracturing wall rock (e.g., Owen et al., 2019, their figure 15), there is no evidence that it played a significant role in the explosivity of the Curacautín ignimbrite eruption (Marshall et al., 2022). The presence of plutonic lithics and mafic to intermediate lavas within the same clasts suggests that autobrecciation and wall-rock rupture and entrainment occurred over depths from 2 km to as shallow as Llaima's ancestral shield ($< 1 \text{ km}$). The abundance of entrained lithics in nearly all clasts also implies mingling across the entire conduit, a process Bamber et al. (2020) attributed to lateral variations in velocity, implying that fusing is not a localized phenomenon (Fig. 4). Alternatively, a narrow conduit from an elongated dike or ring fracture would increase the ratio of surface area to volume, promoting shear across

the conduit and thus pervasive autobrecciation and enabling the dispersal of entrained lithics across the conduit.

Implications for Eruption Interpretation

Bulk properties of fused clasts reflect mingled domains of magma with different vesicularity, permeability, and crystallinity. This presents a challenge for the use of clast-scale data for eruption interpretation, such as using bubble and crystal data to estimate ascent rates and time scales of crystallization. The incorporation and fusing of both lithics and smaller clasts within larger clasts alters densities, obscuring the true nature of the bulk magma. Fused clasts also alter the pre-fused fragmented grain-size distribution, which alters final deposit granulometry (Fig. 2; Giachetti et al., 2021).

Our hypothesis that $l < 10 \mu\text{m}$ plagioclase microlites formed following fusing has

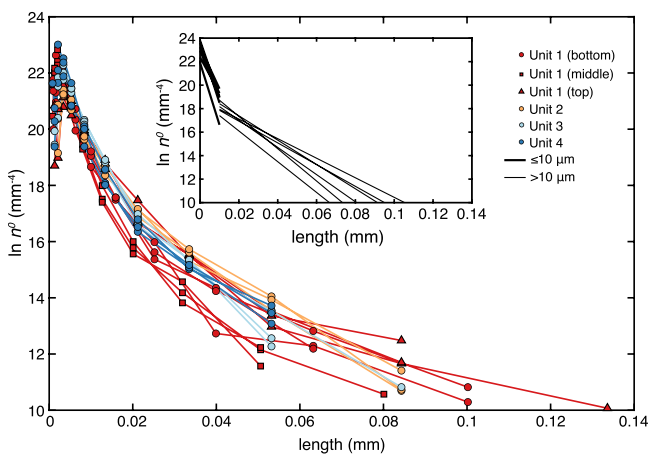


Figure 3. Curacautín (Chile) ignimbrite crystal size distributions from Valdivia et al. (2022) with regressions fit to long axis, $l \leq 10 \mu\text{m}$ and $l > 10 \mu\text{m}$ size populations (inset). n^o is the plagioclase nucleation density. Downturns in crystal size distributions are likely due to the difficulty of intersecting small microlites in two dimensions, and not inadequate imaging resolution (Valdivia et al., 2022), and are not included in regressions. Units 1–4 are the ignimbrite flow units identified by Marshall et al. (2022) (see the Supplemental Material [see footnote 1]).

important implications for crystal size-distribution interpretation. Valdivia et al. (2022) calculated τ of 2–900 s for the smallest plagioclase size fraction using constant nucleation and growth rates, indicating little time between fragmentation and eruption (Fig. 3). Interpreting crystal size distributions with constant microlite nucleation and growth cannot produce reliable time-averaged ascent rates if significant microlite crystallization occurred after fragmentation (e.g., Moore et al., 2022).

While fusing is common in surface flows from effusive mafic eruptions, such as Hawaiian fountains, spatter, or a'a flows, it is not widely documented in the products of highly explosive mafic Plinian and ignimbrite-forming eruptions. Reported instances include the 1886 CE eruption of Tarawera, New Zealand (Sable et al., 2009; Schauroth et al., 2016), the 1918 eruption of Katla, Iceland (Owen et al., 2019), the 11 ka eruption of Tongariro, New Zealand (Heinrich et al., 2020), ignimbrites of the Roman magmatic province (Giordano et al., 2010; Vinkler et al., 2012), and perhaps the 2.1 ka Masaya Triple Layer tephra, Nicaragua (Bamber et al., 2020). Heterogeneous textures of crystalline and glassy domains in clasts of the Croscat eruption, Spain (Cimarelli et al., 2010), are attributed to mingling owing to variable ascent rates across the conduit. Curacautín ignimbrite clasts, however, lack glassy domains, which we interpret as the complete intermingling across the conduit during fusing while the magma was above the glass transition temperature. Broken crystals surrounded by intact melt are typical in clasts from explosive basaltic eruptions, providing an additional record of fragmentation and healing of fractures (Taddeucci et al., 2021). Concomitant degassing can facilitate decompression-induced microlite crystallization in mafic magmas (e.g., Vinkler et al., 2012), and lithics may serve as nucleation sites for new crystals. Together, those processes increase magma viscosity and promote fragmentation.

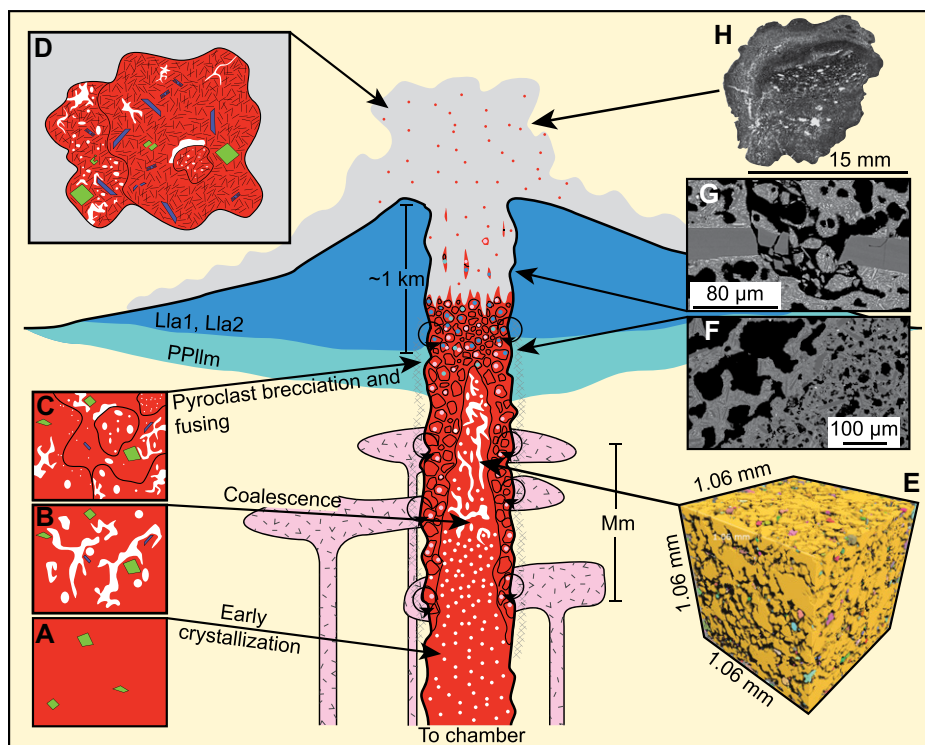


Figure 4. Schematic diagram of our conceptual conduit model for the Curacautín (Chile) ignimbrite eruption. (A) Early crystallization in the reservoir generated 1–3.5 vol% phenocrysts (Marshall et al., 2022) (red polygons are melt, green are early crystals). (B) As Curacautín magma ascended, bubbles nucleated, grew, and coalesced, and new microlites formed (white polygons are vesicles, purple are new crystallization). (C) Magma adjacent to conduit margins autobrecciated and created melt-rich magma particles that were recaptured and fused. Domains of heterogeneous vesicle textures were preserved within individual particles. Miocene plutonic country rocks (unit Mm), Pliocene basaltic to andesitic lavas (unit PP1lm), and Middle Pleistocene ancestral Llaima lavas (units Lla1, LLa2; Naranjo and Moreno, 2005) were incorporated into Curacautín magma prior to fusing. (D) Following fragmentation, rapid (seconds to minutes) microlite crystallization overprinted sutures between fused particles resulting in 84%–94% of the total number of plagioclase microlites in the erupted Curacautín clasts (black lines). The processes in panels A–D occur over many scales. (E) Reconstruction of the Curacautín vesicle network (Valdivia et al., 2022). Yellow domain is a single, interconnected vesicle, and additional colors are smaller, isolated vesicles. (F) Scanning electron microscope (SEM) images of a suture between domains of contrasting vesicle textures overprinted by microlite crystallization. (G) SEM image of shattered phenocryst and microlites from brittle behavior driven by bubble expansion in a shallow conduit. (H) Thin-section scan of a Curacautín ignimbrite clast with heterogeneous vesicle domains. The ubiquity of fusing would be favored by dike-shaped conduits. The nucleation zone for plagioclase with long axis $l \leq 10 \mu\text{m}$ is not quantified here.

CONCLUSIONS

Textures preserved within Curacautín ignimbrite clasts record autobrecciation and particle fusing within Llaima's conduit prior to final fragmentation and eruption. Fused clasts retain heterogeneous vesicle textures overprinted by post-fusing plagioclase crystallization of $l \leq 10 \mu\text{m}$ microlites. Just as sintered obsidian ash records repeated magma brecciation and welding in the conduit, so do fused mafic clasts in the Curacautín ignimbrite. Lithics excavated from conduit margins are fully incorporated into erupted clasts and suggest that brecciation and fusing can occur from a depth of many kilometers up to shallow (<1 km) depths. These observations and interpretations provide insights into conduit conditions preceding and during highly explosive mafic eruptions. The

process of conduit autobrecciation and the role of conduit geometry warrant further exploration through experimental or numerical studies. Care should also be taken when interpreting clast bulk composition and density, vesicle and crystal textures, and granulometry because heterogeneity from fusing would alter these measurements and hence affect interpretations of conduit processes.

ACKNOWLEDGMENTS

Research was supported by National Geographic Foundation grant 9942-12, U.S. National Science Foundation grant EAR-1831143, CIFAR Earth 4D (Canada), and the Alexander von Humboldt Foundation (Germany). Tomography was enabled by Advanced Light Source proposal ALS-09197. We thank T. Giachetti, G. Giordano, an anonymous reviewer, and editor K. Benison for comments, and J. Bowers for scanning thin sections at Oregon State University (Corvallis, Oregon, USA).

REFERENCES CITED

Arzilli, F., et al., 2019, Magma fragmentation in highly explosive basaltic eruptions induced by rapid crystallization: *Nature Geoscience*, v. 12, p. 1023–1028, <https://doi.org/10.1038/s41561-019-0468-6>.

Bamber, E.C., Arzilli, F., Polacci, M., Hartley, M.E., Fellowes, J., Di Genova, D., Chavarria, D., Saballos, J.A., and Burton, M.R., 2020, Pre- and syn-eruptive conditions of a basaltic Plinian eruption at Masaya Volcano, Nicaragua: The Masaya Triple Layer (2.1 ka): *Journal of Volcanology and Geothermal Research*, v. 392, 106761, <https://doi.org/10.1016/j.jvolgeores.2019.106761>.

Carey, R.J., Houghton, B.F., Sable, J.E., and Wilson, C.J.N., 2007, Contrasting grain size and componentry in complex proximal deposits of the 1886 Tarawera basaltic Plinian eruption: *Bulletin of Volcanology*, v. 69, p. 903–926, <https://doi.org/10.1007/s00445-007-0117-6>.

Cassidy, M., Manga, M., Cashman, K., and Bachmann, O., 2018, Controls on explosive-effusive volcanic eruption styles: *Nature Communications*, v. 9, 2839, <https://doi.org/10.1038/s41467-018-05293-3>.

Cimarelli, C., Di Traglia, F., and Taddeucci, J., 2010, Basaltic scoria textures from a zoned conduit as precursors to violent Strombolian activity: *Geology*, v. 38, p. 439–442, <https://doi.org/10.1130/G30720.1>.

Coltelli, M., Del Carlo, P., and Vezzoli, L., 1998, Discovery of a Plinian basaltic eruption of Roman age at Etna volcano, Italy: *Geology*, v. 26, p. 1095–1098, [https://doi.org/10.1130/0091-7613\(1998\)026<1095:DOAPBE>2.3.CO;2](https://doi.org/10.1130/0091-7613(1998)026<1095:DOAPBE>2.3.CO;2).

Constantini, L., Bonadonna, C., Houghton, B.F., and Wehrmann, H., 2009, New physical characterization of the Fontana Lapilli basaltic Plinian eruption, Nicaragua: *Bulletin of Volcanology*, v. 71, 337, <https://doi.org/10.1007/s00445-008-0227-9>.

Cordonnier, B., Caricchi, L., Pistone, M., Castro, J., Hess, K.-U., Gottschaller, S., Manga, M., Dingwell, D.B., and Burlini, L., 2012, The viscous-brittle transition of crystal-bearing silicic melt: Direct observation of magma rupture and healing: *Geology*, v. 40, p. 611–614, <https://doi.org/10.1130/G3914.1>.

Gardner, J.E., Llewellyn, E.W., Watkins, J.M., and Befus, K.S., 2017, Formation of obsidian pyroclasts by sintering of ash particles in the volcanic conduit: *Earth and Planetary Science Letters*, v. 459, p. 252–263, <https://doi.org/10.1016/j.epsl.2016.11.037>.

Giachetti, T., Trafton, K.R., Wiejaczka, J., Gardner, J.E., Watkins, J.M., Shea, T., and Wright, H.M.N., 2021, The products of primary magma fragmentation finally revealed by pumice agglomerates: *Geology*, v. 49, p. 1307–1311, <https://doi.org/10.1130/G48902.1>.

Giordano, G., and The Carg Team, 2010, Stratigraphy, volcano tectonics and evolution of the Colli Albani volcanic field, in Funiciello, R., and Giordano, G., eds., *The Colli Albani Volcano: Geological Society, London, Special Publications of IAVCEI (International Association of Volcanology and Chemistry of the Earth's Interior)* 3, p. 43–97, <https://doi.org/10.1144/IAVCEI003.4>.

Gonnermann, H.M., 2015, Magma fragmentation: *Annual Review of Earth and Planetary Sciences*, v. 43, p. 431–458, <https://doi.org/10.1146/annurev-earth-060614-105206>.

Hammer, J.E., 2004, Crystal nucleation in hydrous rhyolite: Experimental data applied to classical theory: *American Mineralogist*, v. 89, p. 1673–1679, <https://doi.org/10.2138/am-2004-11-1212>.

Hammer, J.E., 2008, Experimental studies of the kinetics and energetics of magma crystallization: *Reviews in Mineralogy and Geochemistry*, v. 69, p. 9–59, <https://doi.org/10.2138/rmg.2008.69.2>.

Heinrich, M., Cronin, S.J., Torres-Orozco, R., Colombier, M., Scheu, B., and Pardo, N., 2020, Micro-porous pyroclasts reflecting multi-vent basaltic-andesite Plinian eruptions at Mt. Tongariro, New Zealand: *Journal of Volcanology and Geothermal Research*, v. 401, 106936, <https://doi.org/10.1016/j.jvolgeores.2020.106936>.

Houghton, B.F., Wilson, C.J.N., Del Carlo, P., Coltelli, M., Sable, J.E., and Carey, R., 2004, The influence of conduit processes on changes in styles of basaltic Plinian eruptions: Tarawera 1886 and Etna 122 BC: *Journal of Volcanology and Geothermal Research*, v. 137, p. 1–14, <https://doi.org/10.1016/j.jvolgeores.2004.05.009>.

Marshall, A.A., Brand, B.D., Martínez, V., Bowers, J.M., Wanless, V.D., Andrews, B.J., Manga, M., Valdivia, P., and Giordano, G., 2022, The mafic Curacautín ignimbrite of Llaima volcano, Chile: *Journal of Volcanology and Geothermal Research*, v. 421, 107418, <https://doi.org/10.1016/j.jvolgeores.2021.107418>.

Moitra, P., Gonnermann, H.M., Houghton, B.F., and Giachetti, T., 2013, Relating vesicle shapes in pyroclasts to eruption styles: *Bulletin of Volcanology*, v. 75, 691, <https://doi.org/10.1007/s00445-013-0691-8>.

Moitra, P., Gonnermann, H.M., Houghton, B.F., and Tiwary, C.S., 2018, Fragmentation and Plinian eruption of crystallizing basaltic magma: *Earth and Planetary Science Letters*, v. 500, p. 97–104, <https://doi.org/10.1016/j.epsl.2018.08.003>.

Moore, H.C., Carey, R.J., Houghton, B.F., Jutzeler, M., and White, J.D.L., 2022, High-temperature oxidation of proximal basaltic pyroclasts, 1886 Tarawera, New Zealand: *Bulletin of Volcanology*, v. 84, 46, <https://doi.org/10.1007/s00445-022-01549-5>.

Naranjo, J.A., and Moreno, H., 2005, Geología del volcán Llaima, Región de la Araucanía: Servicio Nacional de Geología y Minería Carta Geológica de Chile, Serie Geología Básica 88, scale 1:50,000, 33 p.

Owen, J., Shea, T., and Tuffen, H., 2019, Basalt, unveiling fluid-filled fractures, inducing sediment intra-void transport, ephemerally: Examples from Katla 1918: *Journal of Volcanology and Geothermal Research*, v. 369, p. 121–144, <https://doi.org/10.1016/j.jvolgeores.2018.11.002>.

Sable, J.E., Houghton, B.F., Del Carlo, P., and Coltelli, M., 2006, Changing conditions of magma ascent and fragmentation during the Etna 122 BC basaltic Plinian eruption: Evidence from clast microtextures: *Journal of Volcanology and Geothermal Research*, v. 158, p. 333–354, <https://doi.org/10.1016/j.jvolgeores.2006.07.006>.

Sable, J.E., Houghton, B.F., Wilson, C.J.N., and Carey, R.J., 2009, Eruption mechanisms during the climax of the Tarawera 1886 basaltic Plinian eruption inferred from microtextural characteristics of the deposits, in Thordarson, T., et al., eds., *Studies in Volcanology: The Legacy of George Walker*: Geological Society, London, Special Publications of IAVCEI (International Association of Volcanology and Chemistry of the Earth's Interior) 2, p. 129–154, <https://doi.org/10.1144/IAVCEI002.7>.

Schauroth, J., Wadsworth, F.B., Kennedy, B., von Au-lock, F.W., Lavallée, Y., Damby, D.E., Vasseur, J., Scheu, B., and Dingwell, D.B., 2016, Conduit margin heating and deformation during the AD 1886 basaltic Plinian eruption at Tarawera volcano, New Zealand: *Bulletin of Volcanology*, v. 78, 12, <https://doi.org/10.1007/s00445-016-1006-7>.

Sottilli, G., Taddeucci, J., and Palladino, D.M., 2010, Constraints on magma–wall rock thermal interaction during explosive eruptions from textural analysis of cored bombs: *Journal of Volcanology and Geothermal Research*, v. 192, p. 27–34, <https://doi.org/10.1016/j.jvolgeores.2010.02.003>.

Szramek, L., Gardner, J.E., and Larsen, J., 2006, Degassing and microlite crystallization of basaltic andesite magma erupting at Arenal Volcano, Costa Rica: *Journal of Volcanology and Geothermal Research*, v. 157, p. 182–201, <https://doi.org/10.1016/j.jvolgeores.2006.03.039>.

Taddeucci, J., Cimarelli, C., Alatorre-Ibargüengoitia, M.A., Delgado-Granados, H., Andronico, D., Del Bello, E., Scarlato, P., and Di Stefano, F., 2021, Fracturing and healing of basaltic magmas during explosive volcanic eruptions: *Nature Geoscience*, v. 14, p. 248–254, <https://doi.org/10.1038/s41561-021-00708-1>.

Valdivia, P., Marshall, A.A., Brand, B.D., Manga, M., and Huber, C., 2022, Mafic explosive volcanism at Llaima Volcano: 3D x-ray microtomography reconstruction of pyroclasts to constrain shallow conduit processes: *Bulletin of Volcanology*, v. 84, 2, <https://doi.org/10.1007/s00445-021-01514-8>.

Vinkler, A.P., Cashman, K.V., Giordano, G., and Gropelli, G., 2012, Evolution of the mafic Villa Senni caldera-forming eruption at Colli Albani volcano, Italy, indicated by textural analysis of juvenile fragments: *Journal of Volcanology and Geothermal Research*, v. 235–236, p. 37–54, <https://doi.org/10.1016/j.jvolgeores.2012.03.006>.

Vona, A., Romano, C., Dingwell, D.B., and Giordano, D., 2011, The rheology of crystal-bearing basaltic magmas from Stromboli and Etna: *Geochimica et Cosmochimica Acta*, v. 75, p. 3214–3236, <https://doi.org/10.1016/j.gca.2011.03.031>.

Wadsworth, F.B., Llewellyn, E.W., Vasseur, J., Gardner, J.E., and Tuffen, H., 2020, Explosive effusive volcanic eruption transitions caused by sintering: *Science Advances*, v. 6, eaba7940, <https://doi.org/10.1126/sciadv.aba7940>.

White, J.D.L., and Valentine, G.A., 2016, Magmatic versus phreatomagmatic fragmentation: Absence of evidence is not evidence of absence: *Geosphere*, v. 12, p. 1478–1488, <https://doi.org/10.1130/GES01337.1>.

Printed in USA